JACS
JOURNAL OF THE AMERICAN CHEMICAL SOCIETY
Article
pubs.acs.org/JACS

Gas-Phase Studies of Substrates for the DNA Mismatch Repair Enzyme MutY

Anna Zhachkina Michelson,[‡] Aleksandr Rozenberg,[‡] Yuan Tian,[‡] Xuejun Sun,[‡] Julianne Davis,[‡] Anthony W. Francis,[†] Valerie L. O'Shea,[†] Mohan Halasyam,[†] Amelia H. Manlove,[§] Sheila S. David,*[,§,†] and Jeehiun K. Lee*[,‡]

[‡]Department of Chemistry and Chemical Biology, Rutgers, The State University of New Jersey, New Brunswick, New Jersey 08901, United States

[†]Department of Chemistry, University of Utah, Salt Lake City, Utah 84112, United States

[§]Department of Chemistry, University of California, Davis, California 95616, United States

Supporting Information

ABSTRACT: The gas-phase thermochemical properties (tautomeric energies, acidity, and proton affinity) have been measured and calculated for adenine and six adenine analogues that were designed to test features of the catalytic mechanism used by the adenine glycosylase MutY. The gas-phase intrinsic properties are correlated to possible excision mechanisms and MutY excision rates to gain insight into the MutY mechanism. The data support a mechanism involving protonation at N7 and hydrogen bonding to N3 of adenine. We also explored the acid-catalyzed (non-enzymatic) depurination of these substrates, which appears to follow a different mechanism than that employed by MutY, which we elucidate using calculations.

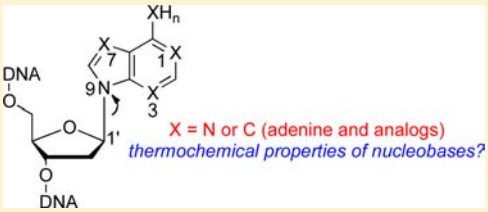

INTRODUCTION

Cellular DNA is inevitably damaged by both exogenous and endogenous agents, resulting in a variety of chemical modifications that are associated with mutagenesis, carcinogenesis, and aging.[1−4] Oxidative damage is extremely prevalent, and one of the most common species formed by reactive oxygen species is 8-oxo-7,8-dihydroguanine (OG).[5−7] During DNA replication, adenine (A) is usually inserted opposite OG to form a relatively stable OG:A mismatch.[8] Because undamaged guanine (G) prefers to pair with cytosine (C), not adenine, the oxidation, if not repaired, can result in permanent G:C→T:A transversion mutations.

In the face of the constant assault to DNA, organisms have developed elaborate DNA repair pathways. In *Escherichia coli*, oxidative damage is repaired by a "GO" repair pathway that utilizes three enzymes: MutT, Fpg, and MutY.[9−11] MutT hydrolyzes the OG deoxynucleoside triphosphate to yield the OG deoxynucleoside monophosphate and pyrophosphate, preventing its incorporation into replicating DNA.[12] Fpg (also called MutM) catalyzes removal of OG from OG:C base pairs, and an associated *β*- and *δ*-lyase activity at the resultant abasic site, leading to strand scission.[1,13] MutY is a somewhat unusual glycosylase enzyme: rather than targeting a damaged base, MutY catalyzes removal of adenine from OG:A mispairs in DNA (Figure 1).[1,12,13] MutY is remarkably specific such that 2′-deoxyadenosine residues within A:T pairs are not touched.

Because of the importance of damaged base repair to genome integrity, the mechanisms of repair enzymes are of great interest.[11] MutY crystal structures, in particular a 2009 *Bacillus stearothermophilus* structure with a fluorinated 2′-deoxyadenosine, show multiple hydrogen-bonding contacts as well as hydrophobic interactions between substrate and enzyme.[14] Kinetic isotope effect studies imply an S_N1-type reaction where the nucleobase leaves (possibly protonated at N7) to yield an oxocarbenium ion which is then attacked by water.[14−16] Recent computational simulations support N7 protonation as well as an active site that organizes solvent to place water molecules into key catalytic positions.[17]

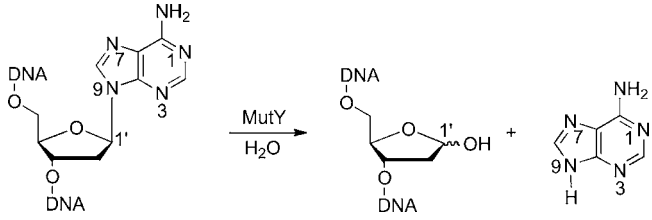

Figure 1. Adenine removal from DNA catalyzed by the MutY glycosylase.

The examination of thermochemical properties in the gas phase, which provides the "ultimate" nonpolar environment, reveals intrinsic reactivity that can be correlated to activity in other media, such as hydrophobic active sites.[18−24] In this paper, we calculate and measure the gas-phase acidities and proton affinities of a series of adenine analogues (not heretofore studied in vacuo) and compare these results to the

Received: September 12, 2012
Published: October 29, 2012

dx.doi.org/10.1021/ja309082k | J. Am. Chem. Soc. 2012, 134, 19839−19850

relative rates of MutY-catalyzed base excision of these analogues within the context of duplex DNA paired with OG. The acid-catalyzed non-enzymatic cleavage of these substrates is also explored.

METHODS

All of the nucleobase analogues (except Z1) and reference acids and bases are commercially available and were used as received. Synthesis of 1-deazaadenosine (Z1) and Z1-containing oligonucleotides was similar to methods previously described; additional details are given in the Supporting Information.[25] Adenine glycosylase assays and acid-catalyzed depurination reactions were also performed as described previously; additional details are provided in the Supporting Information.[26]

The bracketing method was used to measure the gas-phase acidity and proton affinity values. A Fourier transform ion cyclotron resonance (FT-ICR) mass spectrometer with dual cell setup (described previously) was used.[18,19,21,27,28] The magnetic field was 3.3 T; the baseline pressure was 1×10^{-9} Torr. The solid nucleobase analogues were introduced into the cell via a heatable solids probe, while liquid reference acids and bases were introduced via a system of heatable batch inlets. Water was pulsed into the cell and ionized by an electron beam (typically 8 eV (for HO^-) or 20 eV (for H_3O^+), 6 μA, 0.5 s) to generate hydroxide and hydronium ions. Substrate ions were generated by deprotonation or protonation of reference acids or bases (with hydroxide or hydronium ions, respectively) and then selected and transferred from one cubic cell to another via a 2-mm hole in the middle trapping plate. Transferred ions were cooled with pulsed argon gas that allowed the pressure to rise to 10^{-5} Torr. Experiments were conducted at ambient temperature.

The typical protocol for bracketing experiments has been described previously.[18,19,27,29,30] Proton-transfer reactions were conducted in both directions. For example, for Z3 acidity bracketing, hydroxide was used to deprotonate neutral Z3. Deprotonated Z3 was transferred into the adjoining cell, where it was allowed to react with the neutral reference acid AH with known gas-phase acidity. In the opposite direction, the deprotonated reference acid A^- was generated and transferred into the adjoining cell, where it was allowed to react with neutral Z3. The occurrence of proton transfer (efficiency of reaction greater than 10%) is regarded as evidence that the reaction is exothermic (denoted as "+" in the tables). Bracketing experiments are run under pseudo-first-order conditions with the neutral reactant in excess, relative to the reactant ions. Reading the pressure of the neutral compounds from the ion gauges is not always accurate; therefore, we "back out" the neutral substrate pressure from fast control reactions (described previously).[19,22,23,29,31,32]

We also utilized the Cooks kinetic method in a quadrupole (LCQ) ion trap mass spectrometer[33−36] to measure the acidities and proton affinities of adenine analogues. The Cooks kinetic method involves the formation of a proton-bound complex, or dimer, of the unknown and a reference acid or base of known acidity or proton affinity.

The proton-bound dimer ions were generated by electrospray ionization (ESI) of 250 μM solutions of an unknown and a reference acid (or base, for proton affinity measurement). Water−methanol (20%) solution was used as solvent.[37] One drop of acetic acid (for proton affinity measurements) or ammonium hydroxide (for acidity measurements) was occasionally used to promote dimer formation. An electrospray needle voltage of ~4 kV and a flow rate of 25 μL/min were applied. The proton-bound complex ions were isolated and then dissociated by applying collision-induced dissociation (CID); the complexes were activated for about 30 ms. Finally, the dissociation product ions were detected to give the ratio of the deprotonated (or protonated) analyte and deprotonated (or protonated) reference acid. A total of 40 scans were averaged for the product ions.

The dissociation of the proton-bound dimer $[AHB_i]^-$ is depicted in eq 1, where AH is the compound of unknown acidity and B_iH represents a series of reference acids of known acidity. The rate constants k_1 and k_2 are for the two different dissociation pathways.

$$[AHB_i]^- \xrightarrow{k_1} [B_iH] + A^- \qquad [AHB_i]^- \xrightarrow{k_2} [AH] + B_i^- \qquad (1)$$

$$\ln(k_1/k_2) = (1/RT_{eff})(\Delta H_{BiH} - \Delta H_{AH}) \qquad (2)$$

The relationship of these rate constants to ΔH_{acid} is shown in eq 2, where R is the gas constant and T_{eff} is the effective temperature[38] of the activated dimer.[33−36] The ratio of the intensities of the two deprotonated products yields the relative acidity of the two compounds of interest (eq 2), assuming that the dissociation has no reverse activation energy barrier and that the dissociation transition structure is late (and therefore indicative of the stability of the two deprotonated products). These assumptions are generally true for proton-bound systems.[36,39,40]

In order to obtain the acidity of compound AH, the natural logarithm of the relative intensity ratios was plotted versus the acidities for a series of reference acids (B_iH), where the slope is $1/RT_{eff}$ and the y-intercept is $-\Delta H_{AH}/RT_{eff}$. The T_{eff} was obtained from the slope. The acidity of compound AH, ΔH_{AH}, was calculated from either eq 2 or the y-intercept. The same procedure was applied for proton affinity measurements (via formation of positively charged proton-bound dimers).

The gas-phase calculations were conducted at the B3LYP/6-31+G(d) level using Gaussian03 and Gaussian09.[41−45] All the structures were fully optimized in the gas phase, and frequencies were calculated (no imaginary frequencies were found). Acidity and proton affinity values are reported as ΔH at 298 K.

Dielectric medium calculations were done using the conductor-like polarizable continuum solvent model (CPCM, single-point calculations on B3LYP/6-31+G(d) gas-phase optimized structures; UAKS cavity) at B3LYP/6-31+G(d) as implemented in Gaussian03.[46−48] The "total free energy in solution" values are reported, and the solvation free energy of a proton (−264.0 kcal mol^{-1}) is accounted for.[49,50]

RESULTS

Adenine and the synthetically derived analogues studied herein are shown in Figure 2.[26,51,52] 7-Deazaadenine (Z, **1**), 3-deazaadenine (Z3, **2**), and 1-deazaadenine (Z1, **3**) are missing nitrogen at the N7, N3, and N1 positions, respectively (as compared to the parent adenine), and were designed to test the importance of the nitrogen at those positions.[51−53] Substrates Q (**4**), M (**5**), and B (**6**) (with atoms numbered as for adenine, to be consistent) are nonpolar isosteres of adenine.[26,52]

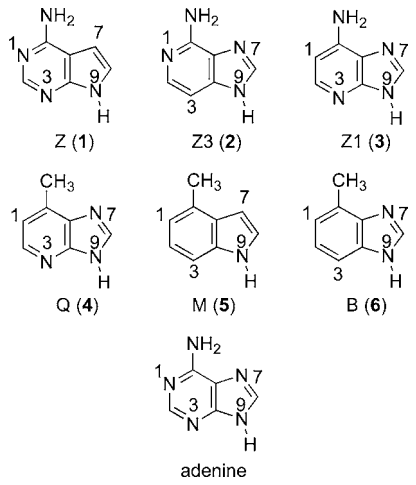

Figure 2. Adenine and synthetic analogues studied herein.

7-Deazaadenine (Z, 1). *1. Calculations: Z Tautomers, Acidity, and Proton Affinity.* In our experience, DFT methods

dx.doi.org/10.1021/ja309082k | J. Am. Chem. Soc. 2012, 134, 19839−19850

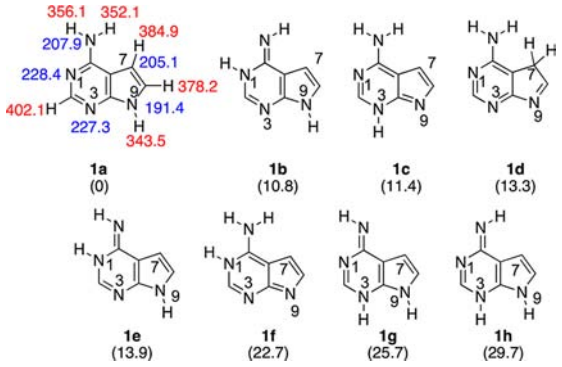

Figure 3. The eight possible tautomeric structures of 7-deazaadenine (Z, **1**). Gas-phase acidities are in red; gas-phase proton affinities are in blue. Relative stabilities are in parentheses. Calculations were conducted at B3LYP/6-31+G(d); reported values are ΔH at 298 K.

Table 1. Summary of Results for Acidity Bracketing of 7-Deazaadenine (Z, 1)

ref compd	ΔH_{acid}[a]	proton transfer[b] ref acid	proton transfer[b] conj base
m-cresol	349.5 ± 2.1	−	+
acetic acid	347.4 ± 0.5	−	+
butyric acid	346.8 ± 2.0	+	+
formic acid	346.0 ± 0.5	+	−
methacrylic acid	344.1 ± 2.9	+	−
methyl cyanoacetate	340.80 ± 0.60	+	−

[a]Acidities are in kcal mol^{-1}.[54,55] [b]A "+" indicates the occurrence and a "−" the absence of proton transfer.

Table 2. Summary of Results for Proton Affinity Bracketing of 7-Deazaadenine (Z, 1)

ref compd	PA[a]	proton transfer[b] ref base	proton transfer[b] conj acid
1-methylpiperidine	232.1 ± 2.0	+	−
1-methylpyrrolidine	230.8 ± 2.0	+	−
piperidine	228.0 ± 2.0	+	+
pyrrolidine	226.6 ± 2.0	−	+
3-picoline	225.5 ± 2.0	−	+

[a]PAs are in kcal mol^{-1}.[54] [b]A "+" indicates the occurrence and a "−" the absence of proton transfer.

generally yield accurate values for thermochemical properties of nucleobases, so we utilized B3LYP/6-31+G(d) to calculate the relative tautomeric stabilities, acidities (ΔH_{acid}), and proton affinities (PA) of 7-deazaadenine (Z, **1**).[18,22,23,29,30] (Throughout the paper, acidity and basicity are calculated only for those tautomers within 10 kcal mol^{-1} of the most stable tautomer.) Z has eight possible tautomeric structures (Figure 3). The most stable tautomer **1a** is over 10 kcal mol^{-1} more stable than the next most stable species. We also calculated the acidity and basicity of the most stable tautomer. The most acidic site of **1a** is predicted to be N9−H (ΔH_{acid} = 343.5 kcal mol^{-1}). The most basic site of tautomer **1a** is N1 (PA = 228.4 kcal mol^{-1}).

2. Experiments: Z Acidity. We measured the acidity of Z using acidity bracketing (details in the Methods section). The conjugate base of Z deprotonates butyric acid (ΔH_{acid} = 346.8 ± 2.0 kcal mol^{-1}); the reaction in the opposite direction (butyrate with Z) also occurs (Table 1). We therefore bracket the ΔH_{acid} of Z as 347 ± 3 kcal mol^{-1}.

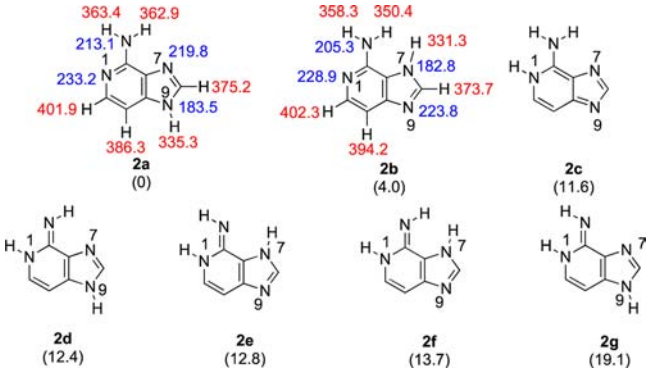

Figure 4. The seven possible tautomeric structures of 3-deazaadenine (Z3, **2**). Gas-phase acidities are in red; gas-phase proton affinities are in blue. Relative stabilities are in parentheses. Calculations were conducted at B3LYP/6-31+G(d); reported values are ΔH at 298 K.

Table 3. Summary of Results for Acidity Bracketing of 3-Deazaadenine (Z3, 2)

ref compd	ΔH_{acid}[a]	proton transfer[b] ref acid	proton transfer[b] conj base
methyl cyanoacetate	340.80 ± 0.60	−	+
trifluoro-*m*-cresol	339.2 ± 2.1	−	+
2-chloropropanoic acid	337.0 ± 2.1	+	+
malononitrile	335.8 ± 2.1	+	−
pyruvic acid	333.5 ± 2.9	+	−
difluoroacetic acid	331.0 ± 2.2	+	−

[a]Acidities are in kcal mol^{-1}.[54] [b]A "+" indicates the occurrence and a "−" the absence of proton transfer.

Table 4. Summary of Results for Proton Affinity Bracketing of 3-Deazaadenine (Z3, 2)

ref compd	PA[a]	proton transfer[b] ref base	proton transfer[b] conj acid
2,2,6,6-tetramethylpiperidine	235.9 ± 2.0	+	−
N,*N*-dimethylcyclohexylamine	235.1 ± 2.0	+	−
triethylamine	234.7 ± 2.0	+	−
di-*sec*-butylamine	234.4 ± 2.0	+	−
1-methylpiperidine	232.1 ± 2.0	−	+
N,*N*-dimethylisopropylamine	232.0 ± 2.0	−	+
1-methylpyrrolidine	230.8 ± 2.0	−	+
piperidine	228.0 ± 2.0	−	+

[a]PAs are in kcal mol^{-1}.[54] [b]A "+" indicates the occurrence and a "−" the absence of proton transfer.

3. Experiments: Z Proton Affinity. In bracketing the PA of Z, we find that piperidine (PA = 228.0 ± 2.0 kcal mol^{-1}) deprotonates protonated Z; the opposite reaction (Z deprotonating protonated piperidine) also occurs (Table 2). We therefore bracket the PA of Z to be 228 ± 3 kcal mol^{-1}.

3-Deazaadenine (Z3, 2). *1. Calculations: Z3 Tautomers, Acidity, and Proton Affinity.* Z3 has seven possible tautomers, of which the most stable is the canonical "N9H" structure **2a** (Figure 4). The "N7H" tautomer **2b** is predicted to be 4 kcal mol^{-1} less stable than **2a**. The gas-phase acidity of **2a** is 335.3 kcal mol^{-1} (corresponding to the N9−H). The most basic site of that tautomer is the N1, with a calculated PA of 233.2 kcal mol^{-1}.

2. Experiments: Z3 Acidity. The acidity of Z3 was measured using the bracketing method (Table 3). We find that

dx.doi.org/10.1021/ja309082k | J. Am. Chem. Soc. 2012, 134, 19839−19850

deprotonated Z3 is able to deprotonate 2-chloropropanoic acid (ΔH_{acid} = 337.0 ± 2.1 kcal mol^{-1}). The reaction in the opposite direction (2-chloropropanoate with Z3) also occurs; we therefore bracket the ΔH_{acid} of Z3 to be 337 ± 3 kcal mol^{-1}.

3. Experiments: Z3 Proton Affinity. The results for the bracketing of the PA of Z3 are in Table 4. We find that di-*sec*-butylamine (PA = 234.4 ± 2.0 kcal mol^{-1}) is able to deprotonate protonated Z3, but that the opposite reaction (protonated di-*sec*-butylamine with Z3) does not occur. 1-Methylpiperidine (PA = 224.7 ± 2.0 kcal mol^{-1}) *cannot* deprotonate protonated Z3, but Z3 can deprotonate protonated 1-methylpiperidine. We therefore bracket the PA of Z3 to be 233 ± 3 kcal mol^{-1}.

1-Deazaadenine (Z1, 3). *1. Calculations: Z1 Tautomers, Acidity, and Proton Affinity.* Z1 has seven possible tautomeric structures (Figure 5). The most stable tautomer **3a** is over 6

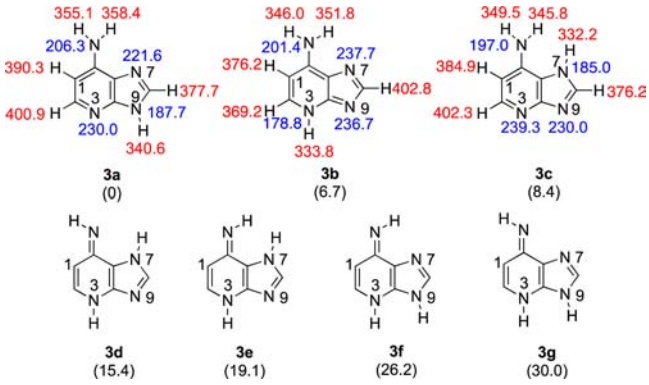

Figure 5. The seven possible tautomeric structures of 1-deazaadenine (Z1, **3**). Gas-phase acidities are in red; gas-phase proton affinities are in blue. Relative stabilities are in parentheses. Calculations were conducted at B3LYP/6-31+G(d); reported values are ΔH at 298 K.

kcal mol^{-1} more stable than the next most stable species. The most acidic site of **3a** is predicted to be the N9 proton (ΔH_{acid} = 340.6 kcal mol^{-1}). The most basic site of tautomer **3a** is the N3 (PA = 230.0 kcal mol^{-1}).

2. Experiments: Z1 Acidity. Efforts to sublime Z1 into the gas phase for acidity and proton affinity bracketing were unsuccessful; we failed to see signal corresponding to the substrate. We were, however, able to measure the acidity and proton affinity using an alternative to bracketing: the Cooks kinetic method (details in the Methods). For the acidity measurement, five reference acids were used (2-fluorobenzoic acid, ΔH_{acid} = 338.0 ± 2.2 kcal mol^{-1}; 3-hydroxybenzoic acid, ΔH_{acid} = 338.6 ± 2.1 kcal mol^{-1}; benzoic acid, ΔH_{acid} = 340.2 ± 2.2 kcal mol^{-1}; phenylacetic acid, ΔH_{acid} = 341.5 ± 2.1 kcal mol^{-1}; and glycine, ΔH_{acid} = 342.7 ± 2.2 kcal mol^{-1}), yielding an acidity (ΔH_{acid}) of 341 ± 3 kcal mol^{-1}.

3. Experiments: Z1 Proton Affinity. We were unable to measure Z1 PA by bracketing (vide supra), but we were able to successfully utilize the Cooks kinetic method. Using guanine (PA = 229.3 ± 2.0 kcal mol^{-1}), *N*-methylpyrrolidine (PA = 230.8 ± 2.0 kcal mol^{-1}), 2,4-lutidine (PA = 230.1 ± 2.0 kcal mol^{-1}), dimethylisopropylamine (PA = 232.0 ± 2.0 kcal mol^{-1}), *N*-methylpiperidine (PA = 232.1 ± 2.0 kcal mol^{-1}), and triethylamine (PA = 234.7 ± 2.0 kcal mol^{-1}) as reference bases, we measure a PA for Z1 of 232 ± 3 kcal mol^{-1}.

"6-Methylated" 1-Deazaadenine (Q, 4). *1. Calculations: Q Tautomers, Acidity, and Proton Affinity.* There are three possible tautomeric structures for Q (Figure 6). The most

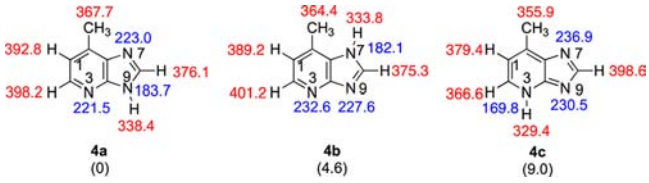

Figure 6. The three possible tautomeric structures of Q (**4**). Gas-phase acidities are in red; gas-phase proton affinities are in blue. Relative stabilities are in parentheses. Calculations were conducted at B3LYP/6-31+G(d); reported values are ΔH at 298 K.

Table 5. Summary of Results for Acidity Bracketing of Q (4)

ref compd	ΔH_{acid}[a]	proton transfer[b] ref acid	proton transfer[b] conj base
formic acid	346.0 ± 0.5	−	+
methacrylic acid	344.1 ± 2.9	−	+
2,4-pentanedione	343.8 ± 2.1	−	+
methyl cyanoacetate	340.80 ± 0.60	+	+
trifluoro-*m*-cresol	339.2 ± 2.1	+	−
2-chloropropanoic acid	337.0 ± 2.1	+	−

[a]Acidities are in kcal mol^{-1}.[54,55] [b]A "+" indicates the occurrence and a "−" the absence of proton transfer.

Table 6. Summary of Results for Proton Affinity Bracketing of Q (4)

ref compd	PA[a]	proton transfer[b] ref base	proton transfer[b] conj acid
1-methylpiperidine	232.1 ± 2.0	+	−
1-methylpyrrolidine	230.8 ± 2.0	+	−
piperidine	228.0 ± 2.0	+	+
pyrrolidine	226.6 ± 2.0	+	+
4-picoline	226.4 ± 2.0	+	+
3-picoline	225.5 ± 2.0	+	+
pyridine	222.3 ± 2.0	−	+
n-octylamine	222.0 ± 2.0	−	+

[a]PAs are in kcal mol^{-1}.[54] [b]A "+" indicates the occurrence and a "−" the absence of proton transfer

stable tautomer **4a** is just over 4 kcal mol^{-1} more stable than the next most stable structure. The most acidic site of **4a** is N9−H, with ΔH_{acid} = 338.4 kcal mol^{-1}. The most basic site is N7, with a PA of 223.0 kcal mol^{-1}.

2. Experiments: Q Acidity. The acidity of Q was bracketed as shown in Table 5. The reaction of deprotonated Q with methyl cyanoacetate (ΔH_{acid} = 340.80 ± 0.60 kcal mol^{-1}) occurs, as does the reverse reaction (deprotonated methyl cyanoacetate with Q). We therefore bracket the acidity of Q as 341 ± 2 kcal mol^{-1}.

3. Experiments: Q Proton Affinity. The proton affinity of Q was bracketed as shown in Table 6. The results are somewhat unusual, in that reaction was found to occur in both directions for reference bases with PAs from piperidine (228.0 ± 2.0 kcal mol^{-1}) to 3-picoline (225.5 ± 2.0 kcal mol^{-1}). The implications of this will be addressed in the Discussion.

"6-Methylated" 1,3,7-Deazaadenine (M, 5). *1. Calculations: M Tautomers, Acidity, and Proton Affinity.* There are two possible tautomeric structures for M, with the more stable being so by over 7 kcal mol^{-1} (Figure 7). The more stable tautomer **5a** has a calculated acidity (at the most acidic site,

dx.doi.org/10.1021/ja309082k | J. Am. Chem. Soc. 2012, 134, 19839−19850

N9−H) of 347.9 kcal mol^{-1}. The PA of the most basic site, C7, is 215.7 kcal mol^{-1}.

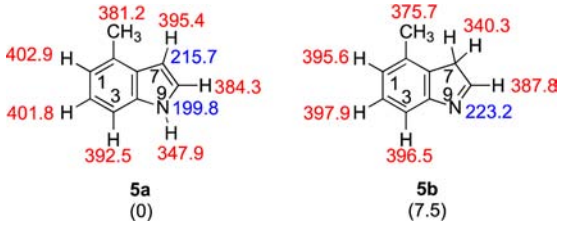

Figure 7. The two possible tautomeric structures of M (**5**). Gas-phase acidities are in red; gas-phase proton affinities are in blue. Relative stabilities are in parentheses. Calculations were conducted at B3LYP/6-31+G(d); reported values are ΔH at 298 K.

2. Experiments: M Acidity. Bracketing experiments with M were hindered by the inability to see any mass spectrometric signal when solid M was heated. However, we were able to vaporize (via electrospray) proton-bound dimers of M with reference acids, allowing us to measure the acidity of M via the Cooks kinetic method. Four reference acids were used (resorcinol, ΔH_{acid} = 346.6 ± 2.1 kcal mol^{-1}; propanoic acid, 347.4 ± 2.2 kcal mol^{-1}; imidazole, 349.9 ± 0.7; and 3-aminophenol, 350.5 ± 2.1 kcal mol^{-1}), yielding an acidity (ΔH_{acid}) of 349 ± 3 kcal mol^{-1}.

3. Experiments: M Proton Affinity. As noted above, bracketing experiments with M were unsuccessful. In addition, measurement of the PA of M by the Cooks kinetic method also failed, as we were unable to form robust signal for proton-bound dimers with reference bases.

"6-Methylated" 1,3-Deazaadenine (B, 6). *1. Calculations: B Tautomers, Acidity, and Proton Affinity.* B has two possible tautomers, both of which are relatively close in stability (Figure 8). The most acidic site of the more stable tautomer **6a** is N9−H (ΔH_{acid} = 339.4 kcal mol^{-1}). The most basic site is N7, with a calculated PA of 228.2 kcal mol^{-1}.

2. Experiments: B Acidity. The acidity of B was bracketed as shown in Table 7. The reaction of deprotonated B with methyl cyanoacetate (ΔH_{acid} = 340.80 ± 0.60 kcal mol^{-1}) occurs; however, deprotonated methyl cyanoacetate cannot deprotonate B. Deprotonated B cannot deprotonate 2,4-pentadione (ΔH_{acid} = 343.8 ± 2.1 kcal mol^{-1}), but deprotonated 2,4-pentadione does deprotonate B. We therefore bracket the acidity of B to be 343 ± 3 kcal mol^{-1}.

3. Experiments: B Proton Affinity. The PA of B was measured using bracketing (Table 8). We find that the reaction with piperidine (PA = 228.0 ± 2.0 kcal mol^{-1}) occurs in both directions (piperidine deprotonates protonated B, and B deprotonates protonated piperidine). We therefore measure the PA of B as 228 ± 3 kcal mol^{-1}.

MutY-Catalyzed Base Excision. Most of the unnatural adenine analogues studied herein (Z, Z3, Q, B, M) have previously been examined as substrates for MutY in DNA duplexes base-paired opposite OG, in order to probe enzymatic mechanistic features.[26,51−53] However, the modified Z1 duplex substrate had not been previously examined and is not commercially available. The appropriate monomer for automated DNA synthesis was synthesized and incorporated into a 30-nucleotide strand (Supporting Information). The glycosylase activity of MutY on a 30-bp duplex containing a central OG:X (X = adenine or adenine analogue) was evaluated as previously reported.[56] Briefly, this involves analyzing the extent

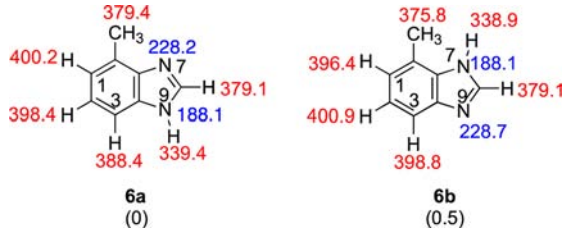

Figure 8. The two possible tautomeric structures of B (**6**). Gas-phase acidities are in red; gas-phase proton affinities are in blue. Relative stabilities are in parentheses. Calculations were conducted at B3LYP/6-31+G(d); reported values are ΔH at 298 K.

Table 7. Summary of Results for Acidity Bracketing of B (6)

		proton transfer[b]	
ref compd	ΔH_{acid}[a]	ref acid	conj base
methacrylic acid	344.1 ± 2.9	−	+
2,4-pentanedione	343.8 ± 2.1	−	+
methyl cyanoacetate	340.80 ± 0.60	+	−
trifluoro-*m*-cresol	339.2 ± 2.1	+	−
malononitrile	335.8 ± 2.1	+	−

[a]Acidities are in kcal mol^{-1}.[54,55] [b]A "+" indicates the occurrence and a "−" the absence of proton transfer.

Table 8. Summary of Results for Proton Affinity Bracketing of B (6)

		proton transfer[b]	
ref compd	PA[a]	ref base	conj acid
1-methylpiperidine	232.1 ± 2.0	+	−
1-methylpyrrolidine	230.8 ± 2.0	+	−
piperidine	228.0 ± 2.0	+	+
pyrrolidine	226.6 ± 2.0	−	+
3-picoline	225.5 ± 2.0	−	+

[a]PAs are in kcal mol^{-1}.[54] [b]A "+" indicates the occurrence and a "−" the absence of proton transfer

of strand scission as a function of time after NaOH quenching of reaction mixtures. Reaction rate constants (k_g) were measured under conditions of single turnover ([MutY] > [DNA substrate]) to remove complications associated with rate-limiting product release. In the case of the OG:Z1-containing duplex, the measured rate constant at 37 °C is 0.3 ± 0.1 min^{-1}. This represents a 40-fold decrease under the same conditions for the reaction of MutY with the corresponding OG:A-containing substrate (k_g = 12 ± 2 min^{-1}). For the series of adenine analogue substrates, the MutY glycosylase activity (k_g), relative to A, is shown in Table 9 (in decreasing order). The substrates are cleaved by MutY in the order A > Q > Z1 > Z3 > B ≫ M = Z.

Acid-Catalyzed Depurination of Adenine Analogue-Containing DNA. Previous work has shown that comparing MutY rates to the susceptibility for acid-catalyzed depurination can reveal insight into features of the enzyme-catalyzed rate. Indeed, previous work with the hydrophobic analogues, B and Q, showed that these analogues are more susceptible to depurination than A.[26] The relative acid-catalyzed depurination of Z1 and Z3 relative to A in the 30-nt oligonucleotide was evaluated using a modified Maxam−Gilbert G+A reaction (Supporting Information). The extent of depurination was quantitated using autoradiography (Figure S1, Supporting Information), and the relative extents of depurination of Z1,

dx.doi.org/10.1021/ja309082k | J. Am. Chem. Soc. 2012, 134, 19839−19850

Table 9. MutY Excision of Nucleobase Analogues Opposite OG within 30 bp DNA Substrates

nucleobase analogue	k_g (min^{-1})[a]	fold reduced relative to OG:A substrate
A	12 ± 2[c]	–
Q (**4**)	1.2 ± 0.2[c]	10×
Z1 (**3**)	0.31 ± 0.06	40×
Z3 (**2**)	0.10 ± 0.05[b]	100×
B (**6**)	<0.002[c]	6000×
M (**5**)	NC[d,e]	>24 000×
Z (**1**)	NC[e]	>24 000×

[a]Rates were measured at 37 °C. Errors represent standard deviation from the average. [b]Value previously reported.[51] [c]Value previously reported.[26] [d]Not cleaved above detection limit (<0.0005 min^{-1}). [e]Value previously reported.[52] [f]Value previously reported.[53]

Z3, and A were normalized to depurination of another A (position 11) within the DNA sequence (Figure S2, Supporting Information). These results show that A, Z1, and Z3 at position 15 are depurinated at fractions of 0.9, 6.3, and 0.3 relative to A11 in the same DNA sequence. Interestingly, this shows that, in contrast to the enzyme-catalyzed excision rates, in acidic water Z1 is depurinated 7 times more than A, whereas depurination of Z3 is 3 times less efficient (Table 10). The trend for acid-catalyzed depurination is Q = Z1 > B >A > Z3.

Table 10. Relative Cleavage of Nucleobase Analogues in Acidic Aqueous Solution

nucleobase	extent of acid-catalyzed depurination (normalized to A)
A	1
Z3	0.3[a]
Z1	7[a]
B	2[b]
Q	7[b]

[a]This work. [b]Values reported previously.[26]

DISCUSSION

Calculated versus Experimental Values. The calculated acidity and proton affinity values for all the substrates studied herein are summarized in Table 11. (The acidity and proton affinity of adenine were previously measured and calculated by us and also appear in the table.) Generally, B3LYP/6-31+G(d) appears to provide fairly accurate predictions for the thermochemical values. The one instance where the calculated and experimental data are quite disparate is for the proton affinity of Q: the calculated value for the most stable tautomer is 223.0 kcal mol^{-1}, yet the bracketing experiment yields a wide range where proton transfer occurs in both directions (PAs from 225.5 to 228.0 kcal mol^{-1}, Table 6). This is a fairly significant discrepancy.

The wide range of proton transfer in both directions for the PA bracketing of Q (Table 6) raises the possibility that, under our conditions, we have a mixture of the two most stable Q tautomers (**4a** and **4b**), and the more basic **4b** (calculated PA of 232.6 kcal mol^{-1}) influences the experimentally observed value. Although the B3LYP/6-31+G(d) calculations indicate that **4b** is nearly 5 kcal mol^{-1} less stable than **4a**, prior studies show that accurate calculations of nucleobase tautomer stabilities can be elusive.[57−61] It is possible that **4b** is less stable than **4a** but perhaps not by as much as the calculations indicate, such that there is some **4b** present in our experiments.

Table 11. Calculated (B3LYP/6-31+G(d); 298 K) and Experimental Data

	substrate	calcd value	exptl value[b]
ΔH_{acid}[a]	Z (**1**)	343.5	347
	Z3 (**2**)	335.3	337
	Z1 (**3**)	340.6	(341)
	Q (**4**)	338.4	341
	M (**5**)	347.9	(349)
	B (**6**)	339.4	343
	adenine	334.8[c]	333 (335)[c]
PA[a]	Z (**1**)	228.4	228
	Z3 (**2**)	233.2	233
	Z1 (**3**)	230.0	(232)
	Q (**4**)	223.0	225.5−228.0
	M (**5**)	215.7	N/A
	B (**6**)	228.2	228
	adenine	223.7[c]	224 (225)[c]

[a]ΔH_{acid} and PA values are in kcal mol^{-1}. [b]Non-parenthetical experimental value is from bracketing measurement; Cooks kinetic method value is in parentheses. Error is ±3−4 kcal mol^{-1}. [c]Values previously reported.[21,22,28.]

For the PA bracketing experiment, the solid **4** is sublimed into the gas phase via a solids probe (typical pressure in the instrument is 10^{-7}−10^{-8} Torr, and the probe is heated to a temperature of roughly 400 K). If only **4a** were present, one would expect a bracketed PA of around 223 kcal mol^{-1}, based on the calculations (Figure 6, Table 11). The bracketing table would have a "crossover point" near pyridine (Table 12).

Table 12. *Hypothetical* Bracketing Table if Only 4a Were Present

		proton transfer	
ref compd	PA	ref base	conj acid
1-methylpiperidine	232.1 ± 2.0	+	–
1-methylpyrrolidine	230.8 ± 2.0	+	–
piperidine	228.0 ± 2.0	+	–
pyrrolidine	226.6 ± 2.0	+	–
4-picoline	226.4 ± 2.0	+	–
3-picoline	225.5 ± 2.0	+	–
pyridine	222.3 ± 2.0	–	+
n-octylamine	222.0 ± 2.0	–	+

If only **4b** were present, one would expect a similar table, except the "crossover point" would be near the PA of the most basic site of **4b**, which is calculated to be 232.6 kcal mol^{-1} (Figure 6). Instead, as can be seen in Table 6, there is not a clean crossover point, but rather a range in which the deprotonation reaction occurs in both directions. We suspect that the reason for this is that both tautomers **4a** and **4b** are present.

In the reactions of a reference base with protonated **4**, if both tautomers were present, then the protonated substrate should be a mixture of $\mathbf{4aH}^+$ and $\mathbf{4bH}^+$ (Figure 9). Under these conditions, any reference base with a proton affinity greater than or equal to 223.0 kcal mol^{-1} should deprotonate **4a**. Consistent with this expectation, we do observe proton transfer for all the reference bases from 3-picoline (PA = 225.5 kcal

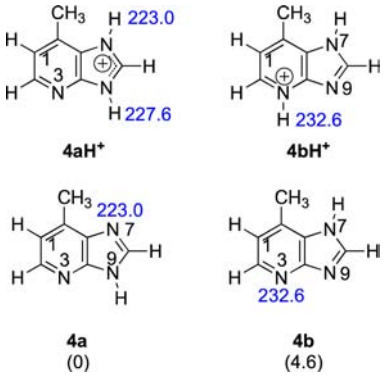

Figure 9. Structures of **4a**, **4b**, **4aH**$^+$, and **4bH**$^+$ and calculated proton affinities. Relative stabilities of the two neutral tautomers are shown in parentheses. Calculations were conducted at B3LYP/6-31+G(d) [ΔH at 298 K in kcal mol^{-1}].

mol^{-1}) to 1-methylpiperidine (PA = 232.1 kcal mol^{-1}, Table 6, "ref base" column).

In the opposite direction, the protonated reference bases are allowed to react with **4**. If both **4a** and **4b** are present, we would expect reaction with any protonated reference base with a PA of about 232 kcal mol^{-1} or less, because **4b** has a calculated PA of 232.6 kcal mol^{-1} (Figure 9). We actually see proton transfer "turn on" at a slightly lower value, 228.0 kcal mol^{-1} (at piperidine; Table 6, "conj acid" column). Still, this value is much higher than the calculated PA of **4a** (223.0 kcal mol^{-1}), pointing to the probable presence of **4b**.

We suspect that the proton transfer "turning on" at a slightly lower value than calculated may be due to a mixture in which **4a** predominates, with less of **4b**. In this bracketing experiment, in order to ascertain whether proton transfer occurs, we measured the kinetics of the proton transfer. We tracked the disappearance of the protonated reference base signal under pseudo-first-order conditions (excess of **4**). We can measure the pressure of **4**, but do not know what percentage of this pressure corresponds to **4b** versus **4a**. Therefore, for those protonated reference bases that only react with **4b**, we measure a rate constant for proton transfer that is less than the actual rate constant, because we can only measure the overall pressure of **4**, but only **4b** reacts. Our PA bracketing results are therefore consistent with a mixture of **4a** and **4b**, with **4a** predominating.

We should also address the bracketed acidity measurement of Q. Tautomer **4a** has a calculated acidity of 338.4 kcal mol^{-1}; tautomer **4b**, 333.8 kcal mol^{-1}. The measured value is 341 kcal mol^{-1}, which implies the presence of tautomer **4a** but not **4b.** However, as we discuss above, we believe both tautomers are present. So why do we measure an acidity consistent with **4a** only?

The deprotonation of both **4a** and **4b** results in the same anion, which is allowed to react with reference acids (Figure 10). This anion should be able to deprotonate any reference

Figure 10. Structure of deprotonated **4a** and **4b** and calculated acidities. Calculations were conducted at B3LYP/6-31+G(d) [ΔH at 298 K in kcal mol^{-1}].

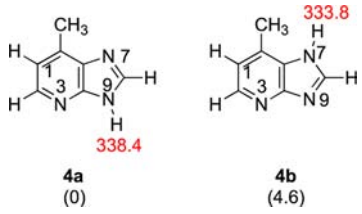

Figure 11. Structures of **4a** and **4b** and calculated acidity of the most acidic site. Relative stabilities of the two neutral tautomers are shown in parentheses. Calculations were conducted at B3LYP/6-31+G(d) [ΔH at 298 K in kcal mol^{-1}].

acid with $\Delta H_{acid} \approx 338$ kcal mol^{-1} or less. Experimentally, we do see proton transfer "turn on" in this region, starting with methyl cyanoacetate (ΔH_{acid} = 340.8 kcal mol^{-1}, Table 5, "ref acid" column).

In the opposite direction, deprotonated reference acids would be allowed to react with **4**, which is presumably a mixture of **4a** and **4b** (Figure 11). In this direction, one would expect to see reaction with any deprotonated reference acid whose ΔH_{acid} is 334 kcal mol^{-1} or higher (since **4b** is present). Instead, however, we do not see proton transfer "turn on" until 340.8 kcal mol^{-1} (Table 5, "conj base" column). We believe that two factors are at play: one, as we saw with the PA experiments, we have less **4b** present, so reactions with **4b** will appear slower than they are. Second, we cannot preclude base-catalyzed tautomerization of **4b** to **4a** taking place during the bracketing experiment (Figure 12; brackets indicate ion–molecule complexes; A$^-$ is the deprotonated reference acid). In Figure 12, we show the reaction of a deprotonated reference acid A$^-$ with **4b**. In this Figure, the reference acid has ΔH_{acid} = 336 kcal mol^{-1}, which is a higher value than the ΔH_{acid} of **4b**, so proton transfer occurs to form deprotonated **4**. However, if a subsequent proton transfer takes place (whereby the N9$^-$ of deprotonated **4**, whose conjugate acid has an acidity of 338.4 kcal mol^{-1}, deprotonates AH), then **4a** and A$^-$ are formed as products (Figure 12). Proton transfer between **4b** and A$^-$ has occurred, but since we only track the m/z ratio of A$^-$, we would have no way of knowing that proton transfer occurred. The exothermic scenario shown in Figure 12 would look, by mass spectrometry, as if no proton transfer has taken place: one would only see A$^-$ signal when following the reaction progress. This would therefore be marked as a "−" in the last column of Table 5, even though proton transfer has occurred. Essentially, therefore, the "−" entries in the rightmost column of Table 5 may actually be incorrect. Thus, the bracketed ΔH_{acid} value of 341 kcal mol^{-1} does not necessarily mean that **4b** is not present.

Given the wide range of proton transfer in both directions for the PA experiment (Table 6) and the ambiguity associated with knowing whether proton transfer occurred in the acidity experiment, we therefore believe that we most likely have a mixture of **4a** and **4b** present under our experimental conditions, with **4a** predominating.

Biological Implications. MutY is a glycosylase that cleaves adenine when it is base-paired to OG. The unnatural substrates studied herein (Z, Z3, Z1, Q, B, M) were synthesized and examined as substrates for MutY, in order to probe enzymatic mechanistic features (most in prior work).[26,51−53] The rates of excision, relative to A, are shown in Table 9 (in decreasing order). The substrates are cleaved by MutY in the order A > Q > Z1 > Z3 > B ≫ M = Z.

dx.doi.org/10.1021/ja309082k | J. Am. Chem. Soc. 2012, 134, 19839−19850

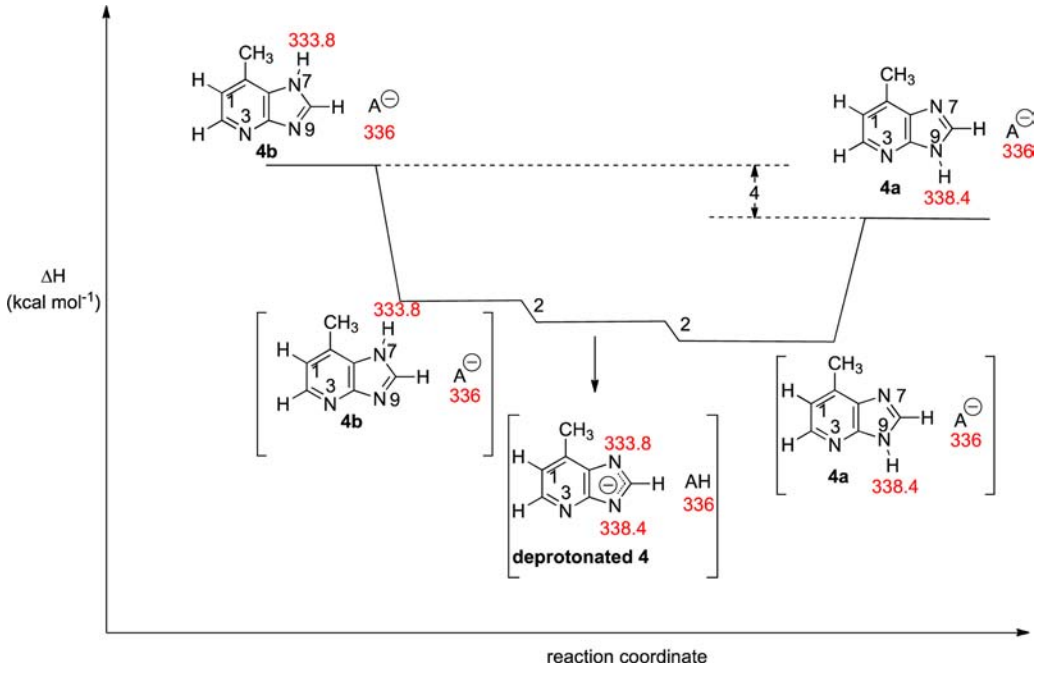

Figure 12. Reaction coordinate for the base-catalyzed tautomerization of **4b** to **4a**. "A^-" represents deprotonated reference acid. Values in red are B3LYP/6-31+G(d) calculated ΔH_{acid} values (298 K).

Scheme 1

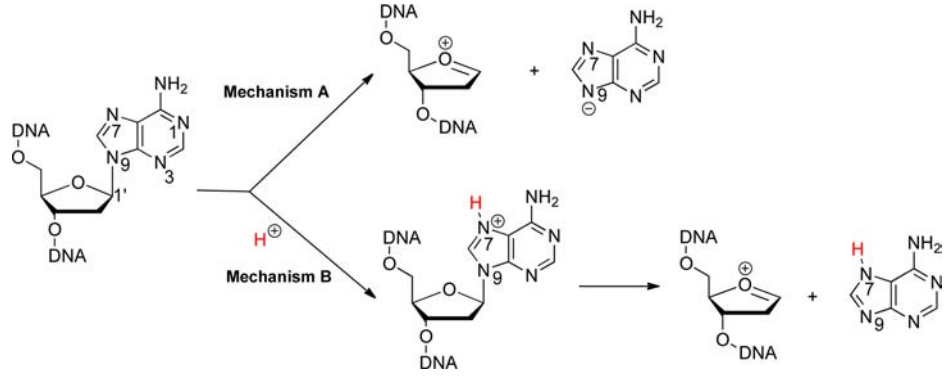

As a key step in initiating DNA repair, BER glycosylases, such as MutY, cleave the *N*-glycosidic bond (Figure 1) to release the damaged or inappropriate base. MutY is a monofunctional glycosylase that hydrolyzes the N-glycosidic bond on 2′-deoxyadenosine to yield an abasic site−DNA product and free adenine base. We are interested in whether the intrinsic properties that we study herein can lend insight into the features used by MutY to catalyze *N*-glycosidic bond breakage. Presumably, the better a leaving group the nucleobase is, the more easily it is cleaved. Since acidity and leaving group ability are generally correlated, we would expect more easily cleaved bases to be more acidic. By examining the intrinsic N9−H acidity for various possible mechanisms, we can lend insight into the operative mechanism. Furthermore, based on our studies with other glycosylases, we postulate that MutY may provide a nonpolar active site that serves to *enhance* the differences in acidity among nucleobases, and in doing so, aids in the discrimination of substrate bases over nonsubstrate bases.[18,19,21,23,62] Thus, studies in the gas phase, which is the ultimate nonpolar environment, are relevant.

Mechanistic studies of MutY, including crystal structure, KIE studies, and computer (molecular dynamics and QM/MM) simulations point to protonation at N7 to facilitate cleavage.[14−17,63] A recent crystal structure of *Bacillus stearothermophilus* MutY bound to a DNA duplex containing a fluorinated 2′-deoxyadenosine paired with OG shows multiple hydrogen bonding contacts as well as hydrophobic interactions between substrate and enzyme.[14,16,63] Glu-43 and Tyr-126 coordinately contact N7; the position of the glutamate indicates that it is probably protonated (the carboxylic acid as opposed to the carboxylate). Glu-43 is expected to be quite acidic, allowing partial or full bonding of its proton to N7. A hydrogen bond from Arg-26 to water to N3 is observed, as well as a hydrogen bond from Arg-31 to N1. Various salt bridges exclude water and create a hydrophobic environment.[14,16,26,51,52]

Acidity: N9−H Acidity of Neutral Nucleobase Analogues. First we considered a mechanism where the *N*-glycosidic bond is simply cleaved without any pre-protonation; in such a scenario, the leaving group is a deprotonated anion (Mechanism A, Scheme 1). In this case, the acidities of the neutral substrates will correlate to their leaving group abilities.

dx.doi.org/10.1021/ja309082k | J. Am. Chem. Soc. 2012, 134, 19839−19850

The calculated (B3LYP/6-31+G(d)) values for the N9−H acidity for the neutral nucleobase analogues are shown in Figure 13. Lower values are more acidic, so adenine is the most

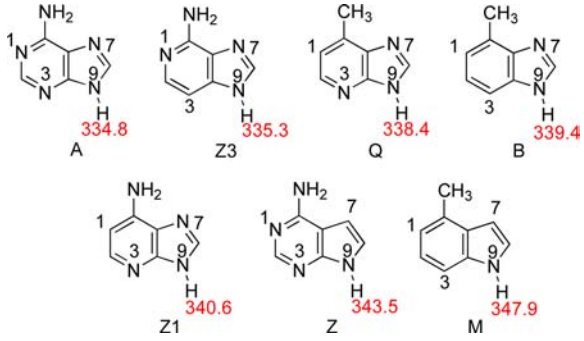

Figure 13. Calculated (B3LYP/6-31+G(d)) gas-phase acidities (ΔH, kcal mol^{-1}) of N9−H for neutral adenine analogues. Substrates are ordered in decreasing acidity (increasing ΔH_{acid} value).

acidic substrate (ΔH_{acid} = 334.8 kcal mol^{-1}).[21,22,61,64−69] The next most acidic substrate is Z3 (ΔH_{acid} = 335.3 kcal mol^{-1}). The trend from most to least acidic in the gas phase is A > Z3 > Q > B > Z1 > Z > M (where A is most acidic). This trend does not agree with the known excision rates for these substrates by MutY (Table 9), which is A > Q > Z1 > Z3 > B ≫ M = Z. Furthermore, the acidity values for Z and M do not seem high enough (relative to the other nucleobases) to explain the experimentally observed lack of excision. Thus, a mechanism where the nucleobases are simply cleaved as anions seems unlikely, at least based on the intrinsic acidity of these substrates. This is not surprising, since most experimental evidence points to pre-protonation at N7 (Mechanism B, Scheme 1).

Acidity: N9−H Acidity of N7-Protonated Substrates. The N9−H acidity values for the N7-protonated nucleobase analogues are shown in Figure 14 (listed in order of increasing acidity). N7-Protonation greatly increases the N9−H acidity (by more than 100 kcal mol^{-1}). The acidity trend is A ∼ Z3 > Q > B > Z1 ≫ Z > M. (The acidities of Z and M without protonation are shown since they lack an N7.)

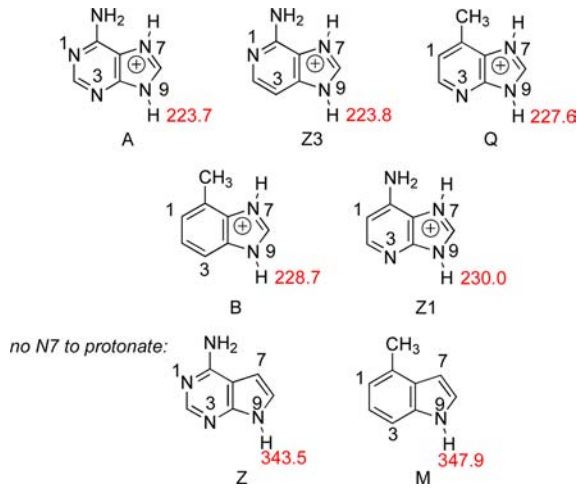

Figure 14. Calculated (B3LYP/6-31+G(d)) gas-phase acidities (kcal mol^{-1}) of N9−H for N7-protonated nucleobase analogues. (Z and M have no N7 to protonate; acidities are shown for comparison.) Substrates are ordered in decreasing acidity (increasing ΔH_{acid} values).

The acidity trend, at first glance, does not correlate to the known excision rates for these substrates by MutY (Table 9, A > Q > Z1 > Z3 > B > M = Z). However, there are some consistencies. M and Z, because of the inability to protonate at N7, are the least acidic by far and would not be expected to be prone to cleavage, which is what is observed experimentally. Q and Z1 are more easily cleaved than would be predicted by the acidities in Figure 14, but both have one feature in common: a nitrogen at N3, which has been proposed to be important for MutY excision.[14,16,26,51]

In order to model the effect of acidity by hydrogen bonding at N3, we used HF as a simple hydrogen-bonding donor.[70] The hydrogen bond at N3 increases the acidity at N9−H of the N7-protonated substrates by roughly 2−3 kcal mol^{-1}. In Figure 15,

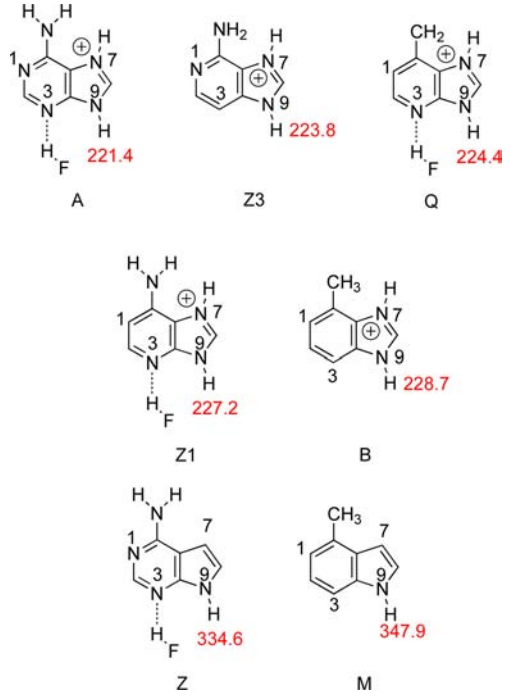

Figure 15. Calculated (B3LYP/6-31+G(d)) gas-phase acidities (kcal mol^{-1}) of N9−H for N7-protonated, N3-hydrogen-bonded adenine analogues. Substrates are ordered in decreasing acidity (increasing ΔH_{acid} values).

we show the gas-phase acidities of the substrates protonated at N7 and hydrogen-bonded to N3 (when N is present at the 7 and 3 positions). The resultant acidity trend is A > Z3 ∼ Q > Z1 > B ≫ Z > M.

This trend compares quite favorably to the actual MutY excision rates (Table 9, A > Q > Z1 > Z3 > B > M = Z). The only substrate "out of place" is Z3, whose gas-phase acidity when protonated at N7 is quite high and implies that Z3 should be prone to cleavage. The reduced ability of MutY to remove Z3 is somewhat of a mystery from the experimental point of view as well; in earlier work one of us postulated that the lack of a N at the 3-position might render N7 more difficult to protonate, which could reduce excision rate. Our gas-phase PA calculations do indicate that Z3 is less basic at N7 than Q and Z1 (Figure 16), so this may explain the observed excision trend.[26,51−53]

dx.doi.org/10.1021/ja309082k | J. Am. Chem. Soc. 2012, 134, 19839−19850

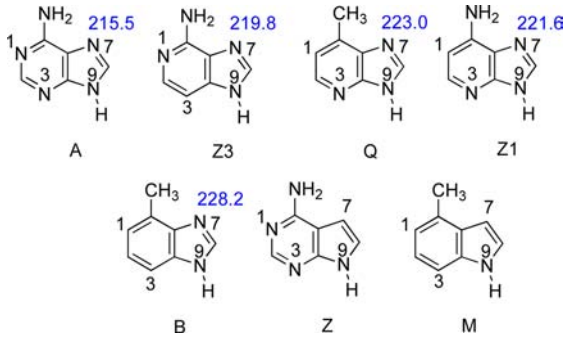

Figure 16. Calculated (B3LYP/6-31+G(d)) gas-phase PAs (ΔH, kcal mol^{-1}) of N7 for adenine and analogues. Substrates are ordered in increasing PA.

Thus, the gas-phase N9−H acidities of these substrates can be compared to known excision rates to lend insight into the MutY mechanism. The gas-phase acidities of the substrates track with excision rates when N7 is protonated and a hydrogen bond is formed to N3, implying that these are features that MutY may provide to enable nucleobase cleavage.

Acid-Catalyzed Non-enzymatic Depurination. We have also studied the nonenzymatic excision of some of these nucleobase analogues in acidic aqueous solution and find a different trend than that for MutY-catalyzed excision. B, Q, and Z1 are depurinated more quickly than A while Z3 is depurinated more slowly (Q = Z1 > B > A > Z3, Table 10).[26] Because this excision trend is different from that catalyzed by MutY, we postulate that the mechanism in acidic aqueous solution is different. Presumably, under acidic conditions, the most basic site of a given nucleobase analogue is protonated, which favors cleavage of the nucleobase. Since the most basic site is not always N7, the acidic aqueous mechanism is different from that of MutY.

To mimic these conditions, relevant calculations should involve pre-protonation of the most basic site and a polar environment. To that end, we calculated the N9−H acidity for the nucleobase analogues when the most basic site is protonated, in a water dielectric (Figure 17). The acidity

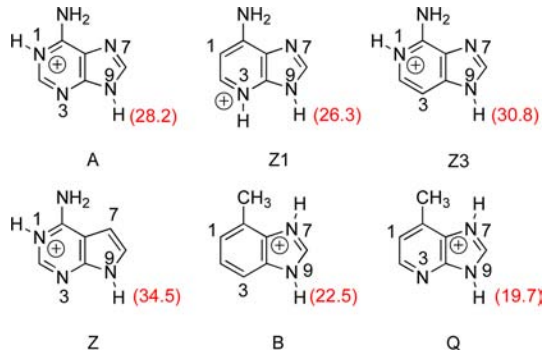

Figure 17. Aqueous N9−H acidities (kcal mol^{-1}) of nucleobase analogues with the most basic site protonated.

values are much lower than those in the gas phase, as would be expected in water. These calculations indicate an N9−H acidity trend of Q > B > Z1 > A > Z3. We would therefore expect Q, B, and Z1 to be cleaved more quickly than adenine, and Z3 to be cleaved more slowly, which is consistent with the experimental results (Table 10). The calculations, which do not include specific solvation, are not perfect; B is predicted to be more quickly cleaved than Z1, but experimentally the opposite is observed. However, the overall trend of which bases should be cleaved more quickly than A and which less quickly is consistent between calculations and experiment, supporting a mechanism in which acid pre-protonates the most basic site prior to cleavage.

1,3-Deazaadenine (Z13) Prediction. One additional substrate we studied computationally is Z13 (Figure 18).

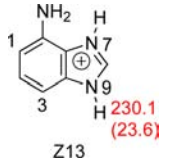

Figure 18. Calculated (B3LYP/6-31+G(d)) gas-phase and (aqueous) acidity (kcal mol^{-1}) of N9−H for N7-protonated nucleobase analogue Z13.

This is a logical extension of the various analogues already studied (Figure 2); this particular derivative is missing an N at both the 1 and 3 positions. Z13 could be a substrate for MutY, although the only nitrogen available for hydrogen bonding and/or protonation is N7. Compared to the other nucleobase analogues, the gas-phase acidity at N9−H when that N7 is protonated is fairly poor (ΔH_{acid} = 230.1 kcal mol^{-1}). Given our hypothesis that N7 is protonated and N3 is hydrogen bonded, the acidity of N9−H of Z13 is even less than that of B (Figure 15). We would therefore expect Z13 to be cleaved by MutY quite slowly, even more slowly than B (but still faster than Z or M).

We also calculated the N9−H acidity for the N7-protonated Z13 in a water dielectric, to predict the ease of acid-catalyzed non-enzymatic depurination. That acidity is 23.6 kcal mol^{-1}, which is more acidic (by 4.6 kcal mol^{-1}) than adenine. We would therefore expect Z13, like Q, B, and Z1, to be cleaved more quickly than adenine under acidic aqueous conditions.

CONCLUSIONS

The heretofore unknown thermochemical properties of adenine and six adenine analogues have been calculated and measured herein. Gas-phase measurements benchmark our calculations. Comparison of the stability of the N9−H bond (in terms of acidity) versus known MutY excision rates point to a MutY-catalyzed mechanism involving protonation at N7, with hydrogen bonding at N3. This conclusion is consistent with other MutY mechanistic studies (crystal structures, kinetic isotope effects). We also find that our calculations for the N9−H acidity when the most basic site is protonated are consistent with experimental data for acid-catalyzed depurination in water. Our work shows that fundamental studies of biological species are valuable for lending insight into mechanisms for which these species are substrates.

ASSOCIATED CONTENT

Supporting Information

Cartesian coordinates for all calculated species, experimental details, acid-catalyzed depurination assays (Figures S1 and S2), and complete refs 44 and 45. This information is available free of charge via the Internet at http://pubs.acs.org.

AUTHOR INFORMATION

Corresponding Author

ssdavid@ucdavis.edu; jee.lee@rutgers.edu

Notes

The authors declare no competing financial interest.

ACKNOWLEDGMENTS

We gratefully thank the NSF, ACS-PRF, NCI/NIH (CA67985), and the National Center for Supercomputer Applications for support. Also, thanks to Mu Chen for valuable discussions and help with the work.

REFERENCES

(1) David, S. S.; Williams, S. D. *Chem. Rev.* **1998**, *98*, 1221−1261.
(2) Lindahl, T. *Nature* **1993**, *362*, 709−715.
(3) Klaunig, J. E.; Kamendulis, L. M. *Annu. Rev. Pharmacol. Toxicol.* **2004**, *44*, 239−267.
(4) Neeley, W. L.; Essigmann, J. M. *Chem. Res. Toxicol.* **2006**, *19*, 491−505.
(5) Shigenaga, M. K.; Park, J.-W.; Cundy, K. C.; Gimeno, C. J.; Ames, B. N. *Methods Enzymol.* **1990**, *186*, 521−530.
(6) Dizdaroglu, M. *Biochemistry* **1985**, *24*, 4476−4481.
(7) Burrows, C. J.; Muller, J. G. *Chem. Rev.* **1998**, *98*, 1109−1152.
(8) McAuley-Hecht, K. E.; Leonard, G. A.; Gibson, N. J.; Thomson, J. B.; Watson, W. P.; Hunter, W. N.; Brown, T. *Biochemistry* **1994**, *33*, 10266−10270.
(9) Cunningham, R. P. *Mutat. Res.* **1997**, *383*, 189−196.
(10) Michaels, M. L.; Tchou, J.; Grollman, A. P.; Miller, J. H. *Biochemistry* **1992**, *31*, 10964−10968.
(11) David, S. S.; O'Shea, V. L.; Kundu, S. *Nature* **2007**, *447*, 941−950.
(12) Michaels, M. L.; Miller, J. H. *J. Bacteriol.* **1992**, *174*, 6321−6325.
(13) Michaels, M. L.; Cruz, C.; Grollman, A. P.; Miller, J. H. *Proc. Natl. Acad. Sci. U.S.A.* **1992**, *89*, 7022−7025.
(14) Lee, S.; Verdine, G. L. *Proc. Natl. Acad. Sci. U.S.A.* **2009**, *106*, 18497−18502.
(15) McCann, J. A. B.; Berti, P. J. *J. Am. Chem. Soc.* **2008**, *130*, 5789−5797.
(16) Fromme, J. C.; Banerjee, A.; Huang, S. J.; Verdine, G. L. *Nature* **2004**, *427*, 652−656.
(17) Brunk, E.; Arey, J. S.; Rothlisberger, U. *J. Am. Chem. Soc.* **2012**, *134*, 8608−8616.
(18) Kurinovich, M. A.; Lee, J. K. *J. Am. Chem. Soc.* **2000**, *122*, 6258−6262.
(19) Liu, M.; Xu, M.; Lee, J. K. *J. Org. Chem.* **2008**, *73*, 5907−5914.
(20) Sun, X.; Lee, J. K. *J. Org. Chem.* **2010**, *75*, 1848−1854.
(21) Sharma, S.; Lee, J. K. *J. Org. Chem.* **2002**, *67*, 8360−8365.
(22) Zhachkina, A.; Liu, M.; Sun, X.; Amegayibor, S.; Lee, J. K. *J. Org. Chem.* **2009**, *74*, 7429−7440.
(23) Sun, X.; Lee, J. K. *J. Org. Chem.* **2007**, *72*, 6548−6555.
(24) Lee, J. K. *Int. J. Mass Spectrom.* **2005**, *240*, 261−272.
(25) DeCarlo, L.; Prakasha Gowda, A. S.; Suo, Z.; Spratt, T. E. *Biochemistry* **2008**, *47*, 8157−8164.
(26) Francis, A. W.; Helquist, S. A.; Kool, E. T.; David, S. S. *J. Am. Chem. Soc.* **2003**, *125*, 16235−16242.
(27) Kurinovich, M. A.; Lee, J. K. *Chem. Commun.* **2002**, 2354−2355.
(28) Sharma, S.; Lee, J. K. *J. Org. Chem.* **2004**, *69*, 7018−7025.
(29) Liu, M.; Li, T.; Amegayibor, S.; Cardoso, D. S.; Fu, Y.; Lee, J. K. *J. Org. Chem.* **2008**, *73*, 9283−9291.
(30) Kurinovich, M. A.; Lee, J. K. *J. Am. Soc. Mass Spectrom.* **2002**, *13*, 985−995.
(31) Chesnavich, W. J.; Su, T.; Bowers, M. T. *J. Chem. Phys.* **1980**, *72*, 2641−2655.
(32) Su, T.; Chesnavich, W. J. *J. Chem. Phys.* **1982**, *76*, 5183−5185.
(33) Cooks, R. G.; Kruger, T. L. *J. Am. Chem. Soc.* **1977**, *99*, 1279−1281.
(34) McLuckey, S. A.; Cameron, D.; Cooks, R. G. *J. Am. Chem. Soc.* **1981**, *103*, 1313−1317.
(35) McLuckey, S. A.; Cooks, R. G.; Fulford, J. E. *Int. J. Mass Spectrom. Ion Phys.* **1983**, *52*, 165−174.
(36) Green-Church, K. B.; Limbach, P. A. *J. Am. Soc. Mass Spectrom.* **2000**, *11*, 24−32.
(37) Fenn, J. B.; Mann, M.; Meng, C. K.; Wong, S. F.; Whitehouse, C. M. *Science* **1989**, *246*, 64−71.
(38) Drahos, L.; Vékey, K. *J. Mass Spectrom.* **1999**, *34*, 79−84.
(39) Ervin, K. M. *Chem. Rev.* **2001**, *101*, 391−444.
(40) Gronert, S.; Feng, W. Y.; Chew, F.; Wu, W. *Int. J. Mass Spectrom.* **2000**, *195/196*, 251−258.
(41) Becke, A. D. *J. Chem. Phys.* **1993**, *98*, 5648−5652.
(42) Lee, C.; Yang, W.; Parr, R. G. *Phys. Rev. B* **1988**, *37*, 785−789.
(43) Kohn, W.; Becke, A. D.; Parr, R. G. *J. Chem. Phys.* **1996**, *100*, 12974−12980.
(44) Frisch, M. J. et al.; *Gaussian 03*; Gaussian, Inc.: Wallingford, CT, 2004.
(45) Frisch, M. J. et al.; *Gaussian 09*; Gaussian, Inc.: Wallingford, CT, 2009.
(46) Barone, V.; Cossi, M. *J. Phys. Chem. A* **1998**, *102*, 1995−2001.
(47) Cossi, M.; Rega, N.; Scalmani, G.; Barone, V. *J. Comput. Chem.* **2003**, *24*, 669−681.
(48) Takano, Y.; Houk, K. N. *J. Chem. Theory Comput.* **2005**, *1*, 70−77.
(49) Tissandier, M. D.; Cowen, K. A.; Feng, W. Y.; Gundlach, E.; Cohen, M. H.; Earhart, A. D.; Coe, J. V.; Tuttle, T. R. *J. Phys. Chem. A* **1998**, *102*, 7787−7794.
(50) Chipman, D. M. *J. Phys. Chem. A* **2002**, *106*, 7413−7422.
(51) Livingston, A. L.; O'Shea, V. L.; Kim, T.; Kool, E. T.; David, S. S. *Nat. Chem. Biol.* **2008**, *4*, 51−58.
(52) Chepanoske, C. L.; Langelier, C. R.; Chmiel, N. H.; David, S. S. *Org. Lett.* **2000**, *2*, 1341−1344.
(53) Porello, S. L.; Williams, S. D.; Kuhn, H.; Michaels, M. L.; David, S. S. *J. Am. Chem. Soc.* **1996**, *118*, 10684−10692.
(54) Hunter, E. P., Lias, S. G. Proton Affinity Evaluation. In *NIST Chemistry WebBook*; Linstrom, P. G., Mallard, W. G., Eds.; NIST Standard Reference Database Number 69; National Institute of Standards and Technology: Gaithersburg, MD; http://webbook.nist.gov (retrieved Aug 28, 2012).
(55) Eyet, N.; Villano, S. M.; Bierbaum, V. M. *Int. J. Mass Spectrom.* **2009**, *283*, 26−29.
(56) Porello, S. L.; Leyes, A. E.; David, S. S. *Biochemistry* **1998**, *37*, 14756−14764.
(57) Wolken, J. K.; Yao, C.; Turecek, F.; Polce, M. J.; Wesdemiotis, C. *Int. J. Mass Spectrom.* **2007**, *267*, 30−42.
(58) Shukla, M. K.; Leszczynski, J. *Chem. Phys. Lett.* **2006**, *429*, 261−265.
(59) Plekan, O.; Feyer, V.; Richter, R.; Coreno, M.; Vallosera, G.; Prince, K. C.; Trofimov, A. B.; Zaytseva, I. L.; Moskovskaya, T. E.; Gromov, E. V.; Schirmer, J. *J. Phys. Chem. A* **2009**, *113*, 9376−9385.
(60) Trygubenko, S. A.; Bogdan, T. V.; Rueda, M.; Orozco, M.; Luque, F. J.; Sponer, J.; Slavicek, P.; Hobza, P. *Phys. Chem. Chem. Phys.* **2002**, *4*, 4192−4203.
(61) Colominas, C.; Luque, F. J.; Orozco, M. *J. Am. Chem. Soc.* **1996**, *118*, 6811−6821 and references therein.
(62) Bennett, M. T.; Rodgers, M. T.; Hebert, A. S.; Ruslander, L. E.; Eisele, L.; Drohat, A. C. *J. Am. Chem. Soc.* **2006**, *128*, 12510−12519.
(63) Guan, Y.; Manuel, R. C.; Arvai, A. S.; Parikh, S. S.; Mol, C. D.; Miller, J. H.; Lloyd, R. S.; Tainer, J. A. *Nat. Struct. Biol.* **1998**, *5*, 1058−1064.
(64) Podolyan, Y.; Gorb, L.; Leszczynski, J. *J. Phys. Chem. A* **2000**, *104*, 7346−7352 and references therein.
(65) Hanus, M.; Kabelac, M.; Rejnek, J.; Ryjacek, F.; Hobza, P. *J. Phys. Chem. B* **2004**, *208*, 2087−2097.
(66) Russo, N.; Toscano, M.; Grand, A.; Jolibois, F. *J. Comput. Chem.* **1998**, *19*, 989−1000.
(67) Huang, Y.; Kenttämaa, H. *J. Phys. Chem. A* **2004**, *108*, 4485−4490.

(68) Chandra, A. K.; Nguyen, M. T.; Uchimaru, T.; Zeegers-Huyskens, T. *J. Phys. Chem. A* **1999**, *103*, 8853−8860.
(69) Del Bene, J. E. *J. Phys. Chem.* **1983**, *87*, 367−371.
(70) We also attempted to use water as the hydrogen bond donor, but calculations were complicated by the propensity of the water proton to hydrogen bond to N9 after deprotonation.